Probabilistic Load Flow for Correlated Wind Power and Storage Usage

Harald Franchetti, BSc., Vienna University of Technology, Vienna, Austria and Carnegie Mellon University, Pittsburgh (PA), USA, November 2011

Abstract

Renewable energies become increasingly important. Wind and solar energy sources are playing a significant role in the field of climate change and smart grid applications. In this research, we focused on wind. We especially looked at the correlation between wind power injections from different wind power plants. Wind power plant output characteristics are known to be β-distributed. We developed a way to model β-distributed random variables with a desired correlation. Our simulation method is DC-load flow. We also took certain line limits into account and used storage devices for storing the energy surplus to avoid overloading the lines. Finally we used actual data to simulate the storage size and initial charge level as well as the state of charge for storage devices located at the injection buses.

1 Introduction

1.1 Motivation

Electricity plays a decisive role in prosperity and technological progress. Since the last centuries electricity has been available to the industry and private households in many of the countries of the world. The generation of electricity in the last centuries was very important to achieve the technological progress but almost the entire electricity production was not environmentally compatible. Worldwide the electricity consumption grows from year to year and the generation becomes more efficient and environmentally friendly. In Fig. 1, we see the outlook for the global electricity consumption

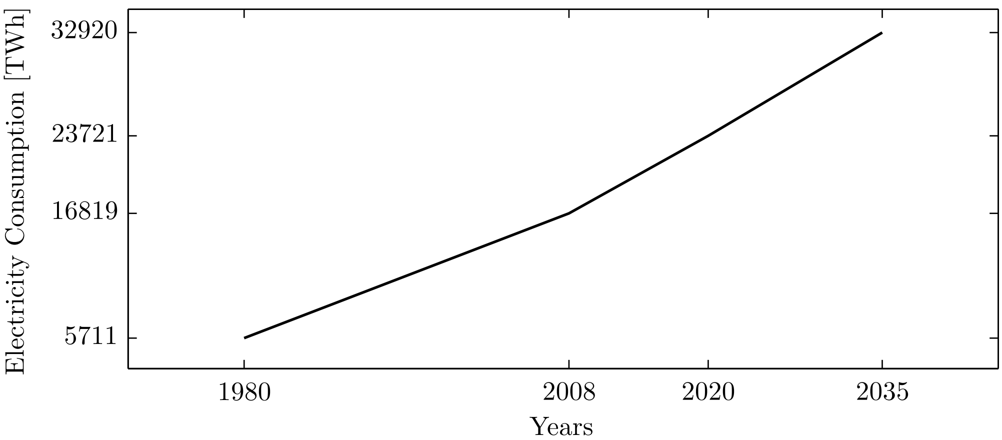

Fig. 1: Global energy consumption outlook 1980-2035 (current policies [1])

up to the year 2035 with respect to the current energy policies [1]. To satisfy this demand we need to build new power plants as well as to increase the efficiency of existing grids and electrical equipment.

Since the discovery of electricity, significant efforts have been put into developing new energy sources. Most used resources are fossil fuels such as coal, oil and natural gas as well as water and nuclear power. Due to oil crises, various nuclear power plant incidents and the present discussion about the climate change, renewable energy resources become more and more important and obtain more public acceptance and support. Wind and solar power are the strongest rising renewable energies. In Fig. 2, we show the cumulative installed capacity on wind power worldwide for the time frame 1996 to 2010 [2] and it is going to continue growing.

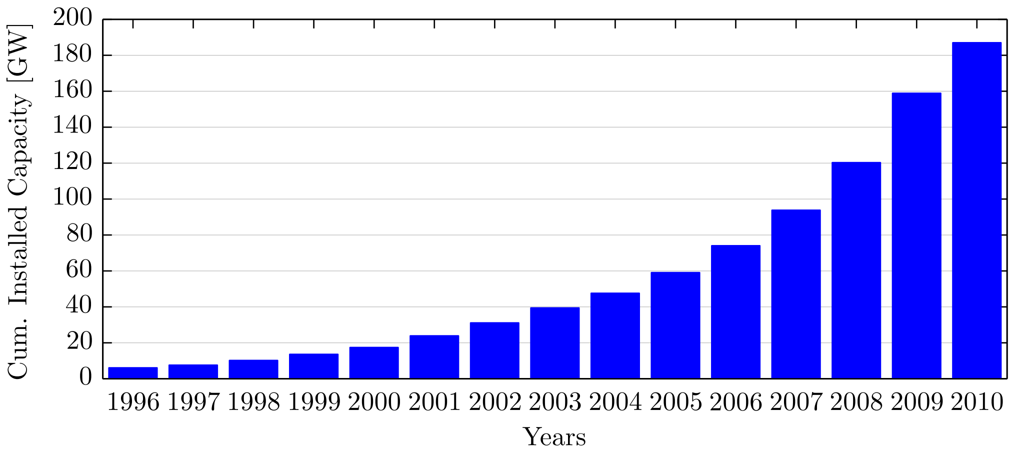

Fig. 2: Global cumulative installed wind capacity 1996-2010 [2]

1.2 Problem Statement

Large amounts of electrical energy cannot be stored directly. We also cannot bottle, sack or bag electrical energy to transport it. This means electrical energy only can be transmitted in suitable amounts through wiring. For a stable and reliable grid it is essential that the sum of generated power has to be exactly equal to the sum of consumed power at each instant of time.

If more power is generated than consumed the frequency of the grid increases as a result of physical laws. On the other hand, if not enough power is produced the frequency goes down. Monitoring the frequency is the best way to observe the power balance of the power grid. During normal operation, the bandwidth of frequency variations are within a few per mill because of continuous variations in load. As soon as the deviation increases, the transmission grid operator has to counteract. This means that the generation has to be increased or reduced regarding to the frequency trend. Equivalent changes to load can also be applied by connecting or disconnecting some loads.

The load can be predicted with high accuracy based on historical measurements but imbalances between supply and demand are inevitable. There are different types of operating reserve to recover equilibrium. These reserves are available from seconds for small amounts and up to several minutes for larger amounts of energy. With help of this balancing power the daily operation is guaranteed.

The accuracy of forecasting wind speed and solar radiation is not as good as required. Wind energy is the kinetic energy of moving air. It is converted to wind power by wind turbines. This kinetic energy can be calculated based on a mass element $\mathrm{d}m$ and the wind velocity v of a volume of moving air that passes through the surface A [3]

$$\mathrm{d}E = \frac{1}{2}\,\mathrm{d}m\,v^2 = \frac{1}{2}\,\rho A v^3 \mathrm{d}t. \tag{1}$$

The wind power that can be transformed into mechanical power to produce electricity can be derived to

$$p = \frac{1}{A}\frac{\mathrm{d}E}{\mathrm{d}t} = \frac{1}{2}\,\rho v^3. \tag{2}$$

The wind power is proportional to the third power of wind velocity. This means the error between predicted and effective wind speed causes a deviation of predicted power that is to the power of three higher than the error itself.

Currently, the amount of intermittent renewable energies for electricity generation worldwide is still small. There is enough operation reserve distributed throughout the grid to deal with the power and frequency variations. But we need more energy generated by environmental-friendly technologies to limit and counter the climate change. Worldwide we see a trend of intense expansion of renewable energies. The whole world is subject to these changes and considerations. A study by Harvard University shows that worldwide is enough wind capacity available to cover more then 40 times the current global electricity consumption [4]. A lot of research and development is ongoing and much more is needed to have secure and reliable technologies for the future applications and operations.

1.3 Contributions of this Research

World climate change is one of the most important and omnipresent topics in power systems today. It is very important to look at unsolved issues with regards to renewable energies and to find solutions to this issues as well as more efficient technologies. Every development and improvement is a necessary step for a more environmental-friendly energy system, starting from generation to transmission to consumption.

The focus in our research is set on probabilistic load flow (PLF) for correlated wind power plant outputs. Since 1974, as Borkowska proposed the PLF-method for the first time [5], this method has been further developed [6]. Inputs for PLF simulations are probability density functions (PDFs) or cumulative distribution functions (CDFs) of power injections and loads. Outputs are also PDFs or CDFs of all branches. We decided to use PDF for our simulations. The relative frequency of occurrence of load values can be seen directly when using PDF. The simulations are solved numerically by using random variables with a specific distribution. This numerical method is known as Monte Carlo.

The probability densities for wind park power outputs often can be described as a Beta distribution [7, 8]. For two or more wind power plants, the influence of wind on these power plants can be modeled as a correlation between their power outputs with respect to their geographical distance to each other.

For PLF with correlated gaussian distributions and PLF without correlation, many different methods are available. Information on correlated and non-gaussian distributed characteristics are very rare and this issue is an object of research.

For two or three wind park outputs with specific β-distributed density function we can generate random variables with the required distribution and a desired correlation in the range from zero to one, if the correlation is possible. For two variables we can see how the distribution transforms from no to a total correlation and vice versa.

As second important part, besides the correlation, we introduced storage units into our model. On each bus where a wind power injection is connected we located a storage unit. This storage facility will be used to optimize the power transfer from the generation to the load and avoid overloaded lines.

We can simulate different types of storage usage for optimization. This includes the combination of storage and wind power injection to provide a net injection to the grid that follows the load for a specific time frame as from five minutes to one year. For this simulation we used real data with a resolution of five minutes. That is the reason why we have five minutes as lower bound. Our data set covers one year. That is the upper bound for our simulations.

We also can run the simulation to get a constant net injection as result. Of course, we also have the same flexibility regarding the time frames for simulating. With these results we see what size of storage we would need if we balance out the variations of wind generations directly at the injection bus or a specific window of time. With real data we also can see what the states of charge of the batteries are. The amount of energy that has to be charged at the beginning is also a part of the simulations results.

Additionally, with a storage unit at each end of a line we also can take certain line limits into account. We just looked at a limit at the last line in a path. No consecutive limited lines are considered. We see then how the probability density changes on the line if a line limit is combined with storage units.

2 Correlated Wind Power Output

As already mentioned the distribution of a wind farm power output typically has a β-characteristic. In this section we introduce the Beta distribution and the linear correlation between two β-distributed random variables as the composition of two or more γ-distributed random variables.

2.1 β-Distribution

The standard β-distribution [9] on interval $[0,1]$ is:

$$f(x,\alpha,\beta) = \frac{1}{\mathrm{B}(\alpha,\beta)} x^{\alpha-1}(1-x)^{\beta-1} \quad x \in [0,1];\ \alpha,\beta > 0 \tag{3}$$

with Beta function

$$\mathrm{B}(\alpha,\beta) = \frac{\Gamma(\alpha)\Gamma(\beta)}{\Gamma(\alpha+\beta)} = \int_0^1 u^{\alpha-1}(1-u)^{\beta-1}\mathrm{d}u \tag{4}$$

where α and β are the shape parameters of the distribution. By applying the transformation

$$x = \frac{x'-a}{b-a} \tag{5}$$

we obtain the β-distribution for the interval $[a,b]$:

$$f(x',a,b,\alpha,\beta) = \frac{1}{\mathrm{B}(a,b,\alpha,\beta)}(x'-a)^{\alpha-1}(b-x')^{\beta-1} \quad x' \in [a,b];\ \alpha,\beta > 0 \tag{6}$$

with Beta function

$$\mathrm{B}(a,b,\alpha,\beta) = \frac{\Gamma(\alpha)\Gamma(\beta)}{\Gamma(\alpha+\beta)}(b-a)^{\alpha+\beta-1} = \int_a^b (u-a)^{\alpha-1}(b-u)^{\beta-1}\mathrm{d}u. \tag{7}$$

2.2 Linear Correlation

We need a measure for the degree of association between two random variables to be able to make a statement about their relationship. This measure must be independent from any units. The covariance is dependent on units and therefore it is not the right choice.

The coefficient of a linear correlation is defined as the fraction of covariance and the product of the variances of the random variables. This coefficient is also called correlation coefficient [10]

$$\rho = \rho_{X,Y} = \mathrm{Corr}(X, Y) = \frac{\mathrm{Cov}(X, Y)}{\sigma_X \sigma_Y}. \tag{8}$$

If the correlation is zero the random variables are uncorrelated but they do not have to be independent. On the other side, independent random variables are definitely uncorrelated.

2.3 Correlated β-Distributed Random Variables

There are different methods to generate correlated β-distributed random variables. We can group them into two main groups. In the first approach, correlated uniform distributed random variables are generated first and then transformed into β-distributions. This is used in many fields as we can see e.g. in [11, 12]. This method produces some bias which cannot really be avoided. The second major approach is to compose two or more γ-distributed random variables to a β-distributed one (for instance [13, 14]) e.g.

$$V = \frac{U_1}{U_1 + U_2}. \tag{9}$$

$$\left.\begin{aligned} U_1 &\sim \mathcal{G}(\gamma_1, \lambda) \\ U_2 &\sim \mathcal{G}(\gamma_2, \lambda) \end{aligned}\right\} V \sim \mathcal{B}(\gamma_1, \gamma_2) \tag{10}$$

The symbol $\sim$ stands for *distributed as* and $\mathcal{G}(\gamma, \lambda)$ or $\mathcal{B}(\gamma_1, \gamma_2)$ denotes a γ-distribution with shape parameter γ and scale parameter λ, and a β-distribution with scale parameters γ_1 and γ_2, respectively.

Magnussen [14] also used the well known additivity of γ-distributed random variables

$$W = U_1 + U_2 \tag{11}$$

$$\left.\begin{aligned} U_1 &\sim \mathcal{G}(\gamma_1, \lambda) \\ U_2 &\sim \mathcal{G}(\gamma_2, \lambda) \end{aligned}\right\} W \sim \mathcal{G}(\gamma_1 + \gamma_2, \lambda) \tag{12}$$

for the correlation. He introduced shared γ-variables as the correlation part of two β-variables like

$$Y_1 = \frac{X_1 + X_a}{X_1 + X_a + X_2 + X_b} \tag{13}$$

$$Y_2 = \frac{X_3 + X_a}{X_3 + X_a + X_4 + X_b}. \tag{14}$$

X_a and X_b are shared variables added to (9) to obtain the desired correlation. These variables are calculated from all shape parameters and the correlation.

In our simulation we used this method. We generated correlated β-distributed random variables from 0 % to 100 % correlation in 10 % steps and summed them

$$Z = Y_1 + Y_2 \tag{15}$$

with $Y_1 \sim \mathcal{B}(\alpha_1, \beta_1)$ and $Y_2 \sim \mathcal{B}(\alpha_2, \beta_2)$.

From results of the simulations with respect to this method with shape parameters $\alpha_1 = 0.87$ and $\beta_1 = 1.23$ for the first and $\alpha_2 = 0.87$ and $\beta_2 = 1.23$ for the second β-distribution can be concluded that the shape parameters α and β are too small for this method to achieve the desired correlations. The values of the achieved correlations are a bit more as half of what they should be (e.g. 26 % instead of 50 % or 55 % instead of 100 %). Tests with larger parameters achieve the right correlation levels.

This effect is well known in signal processing and is called bias. In the derivation of this method, Magnussen uses a first-order Taylor series expansion. This approximation may cause the bias. A bias larger than 10 % may be restricted to β-distributions with near exponential or exponential-types. But in general, the bias is larger the smaller the parameters α and β are. For applications describing wind power output characteristics, usually parameters less than 5 are used.

We noticed that this method has great capabilities and we adopted it for our needs. The issue is the calculation of the shared variables and we developed a method that works for our simulations.

For positive correlation we calculate our shared variables X_a and X_b by

$$X_a \sim \mathcal{G}(\rho \cdot \max(\alpha_1, \alpha_2), \lambda) \tag{16}$$

$$X_b \sim \mathcal{G}(\rho \cdot \max(\beta_1, \beta_2), \lambda) \tag{17}$$

and for a negative correlation

$$X_a \sim \mathcal{G}(\rho \cdot \max(\alpha_1, \beta_2), \lambda) \tag{18}$$

$$X_b \sim \mathcal{G}(\rho \cdot \max(\beta_1, \alpha_2), \lambda). \tag{19}$$

In Fig. 3, this method was applied in our simulations. We tested the same configuration, two β-distributions with shape parameters α_1, β_1 and α_2, β_2 and looked at the correlation in 10 % steps for the power output.

The achieved correlation is pretty good but it still has a small bias. Now we can see the transformation of the sum from the case of the independent random variables to totally correlated or identical variables. The light blue curve is the calculated result of the convolution of the two probabilistic density functions (PDFs) of the independent random variables. The black curve is the original source PDF and it is the same as 100 % correlation.

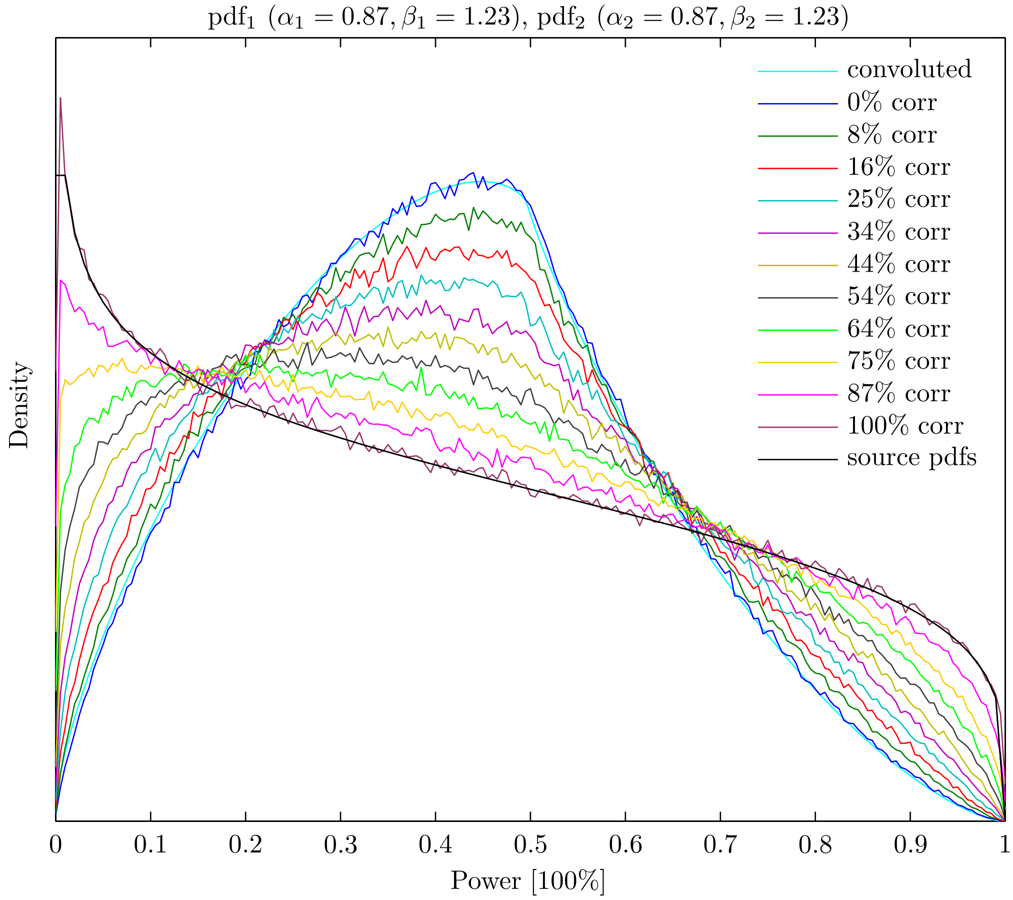

Fig. 3: Positive correlation and distributions with same shape

In Fig. 4, we show the simulation result for a contrary shape ($\alpha_2 = \beta_1$ and $\alpha_2 = \beta_1$) of the β-distributions with positive correlation. With this difference in shape only about 77 % of correlation is possible.

In Fig. 5 and Fig. 6, the same simulations are shown but with negative correlation. Here, of course, a totally correlation is possible for contrary shapes and for the same shape only about 77 %. The term NaN stands for *Not a Number* and this means the result during the simulation is not valid.

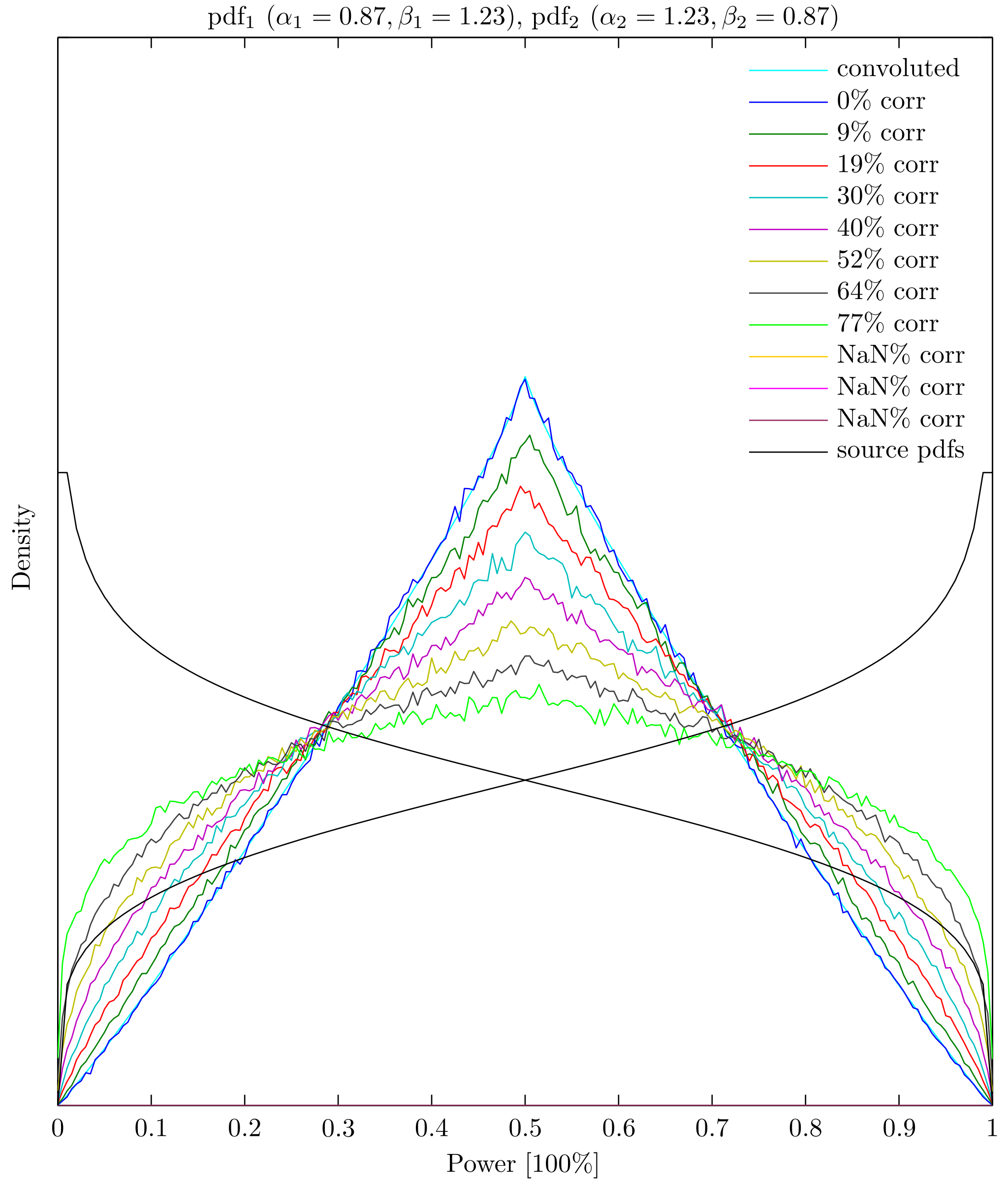

Fig. 4: Positive correlation and distributions with contrary shape

A correlation of 80 %, 90 % or 100 % cannot exist in this case. For a total correlation the PDF is only a peak at zero.

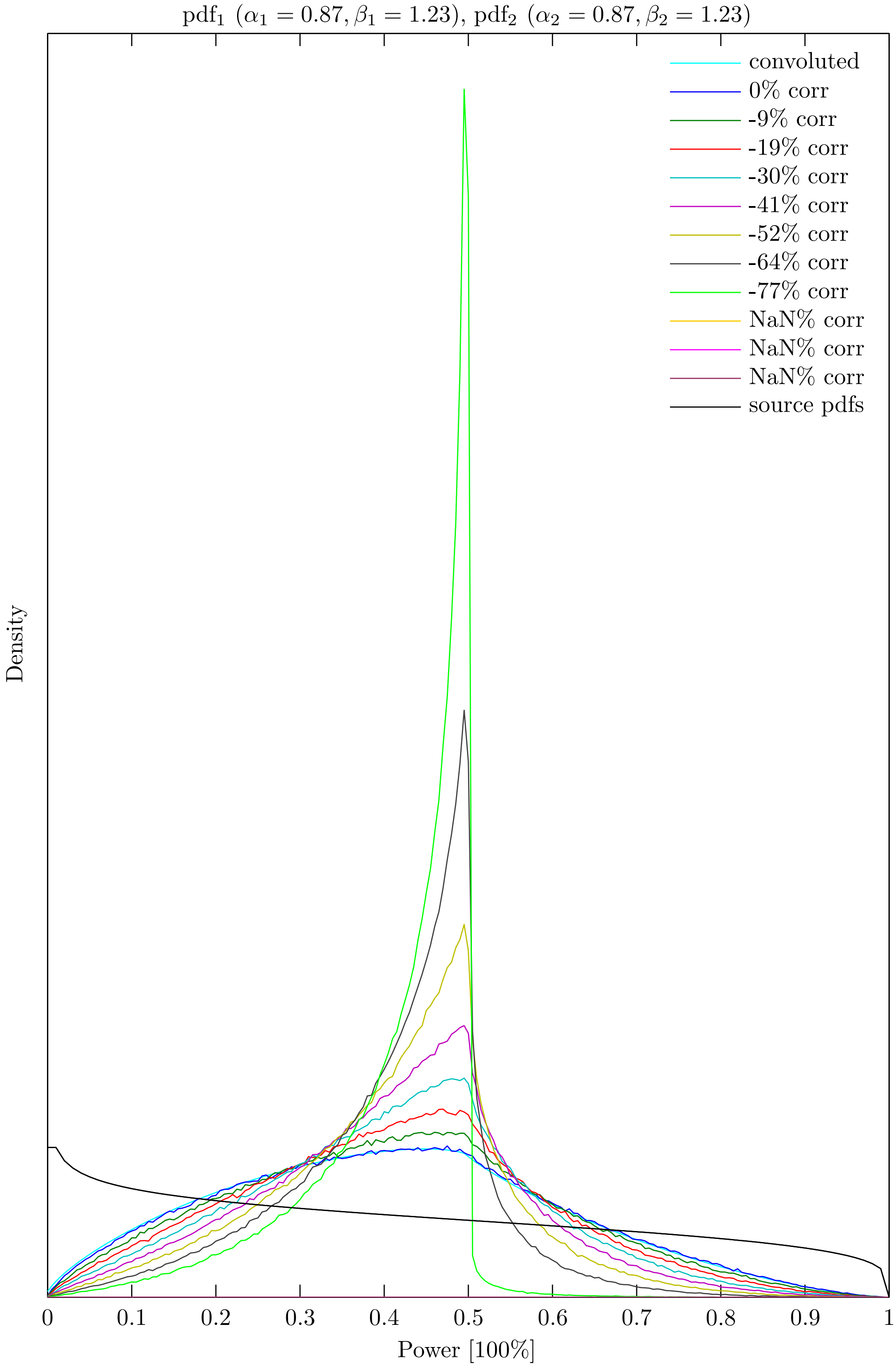

Fig. 5: Negative correlation and distributions with same shape

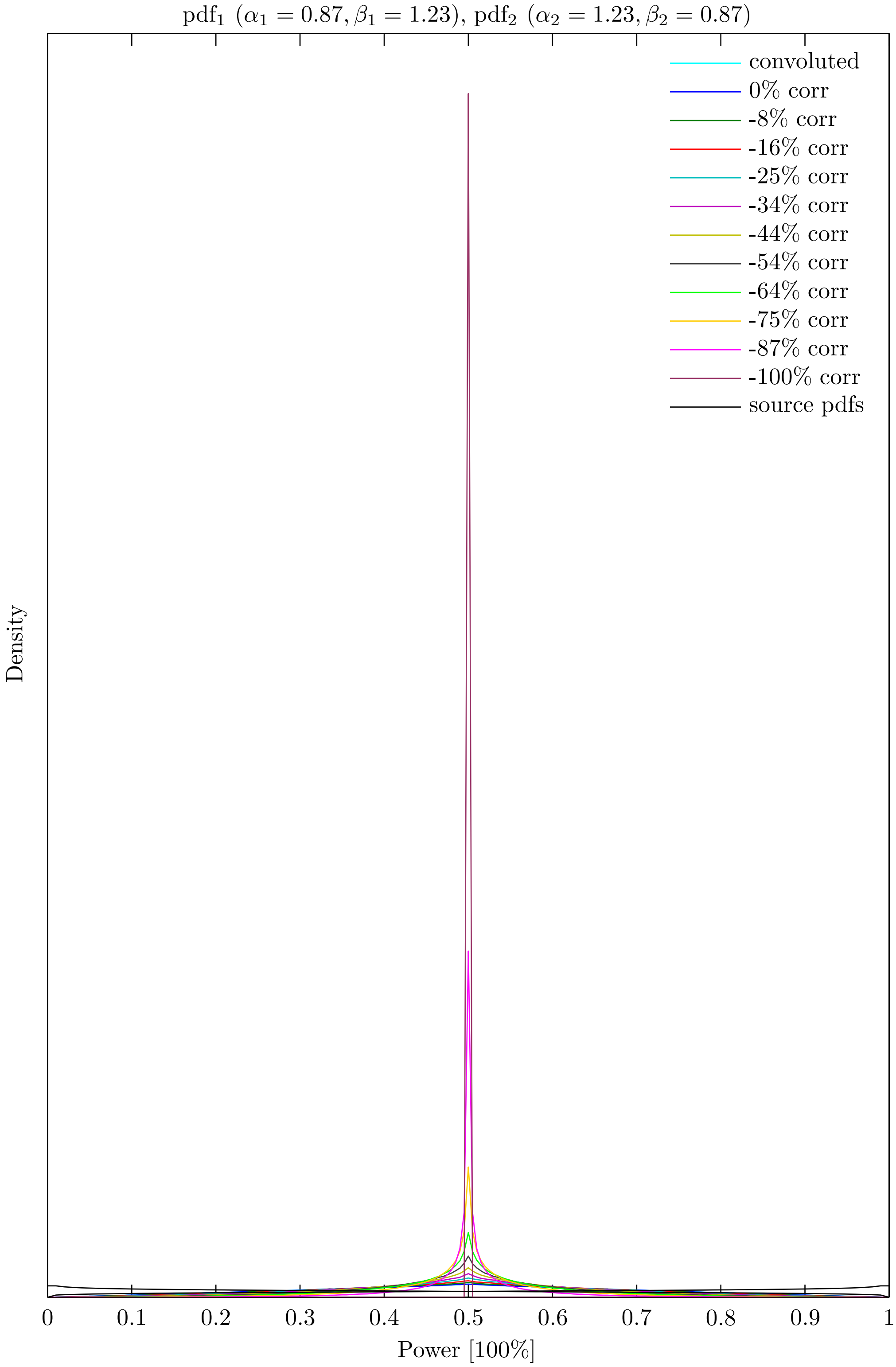

Fig. 6: Negative correlation and distributions with contrary shape

2.4 Correlation Compensation

Especially for the same shape and the positively correlated case we worked on a perfection of the proposed correlation method. Negative correlation as well as shapes with parameters where $\alpha > \beta$ are not so important for the application to wind farms. We measured the bias and developed an algorithm for compensation.

In Fig. 7, a biased and the corresponding desired characteristics are shown. With this compensation diagram we are able to generate almost perfectly positively correlated β-distributed random variables with a specific correlation between 0 % and 100 % for the same shape of the distributions. We also ran the simulation and the result can be seen in Fig. 8. The corre-

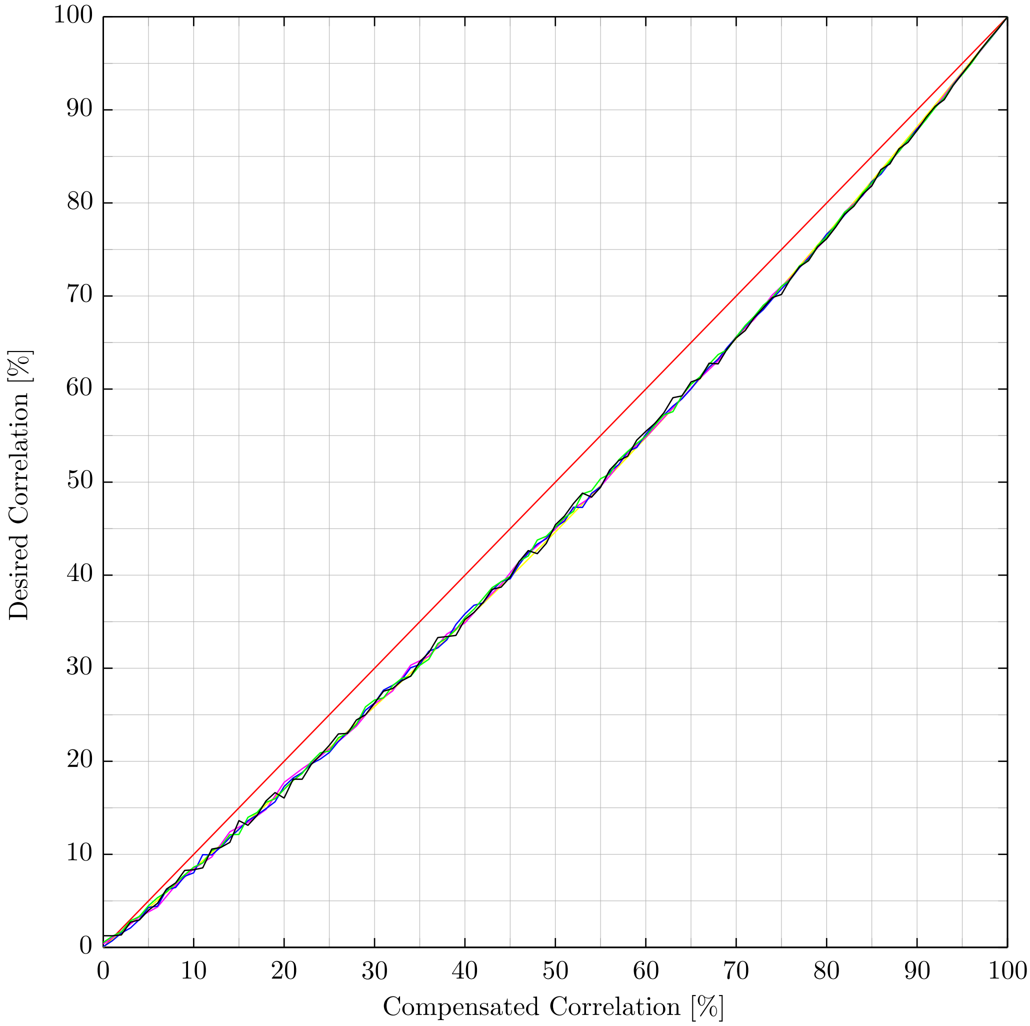

Fig. 7: Correlation characteristic of generated β-distributed random variables

lation values are rounded at the first decimal place.

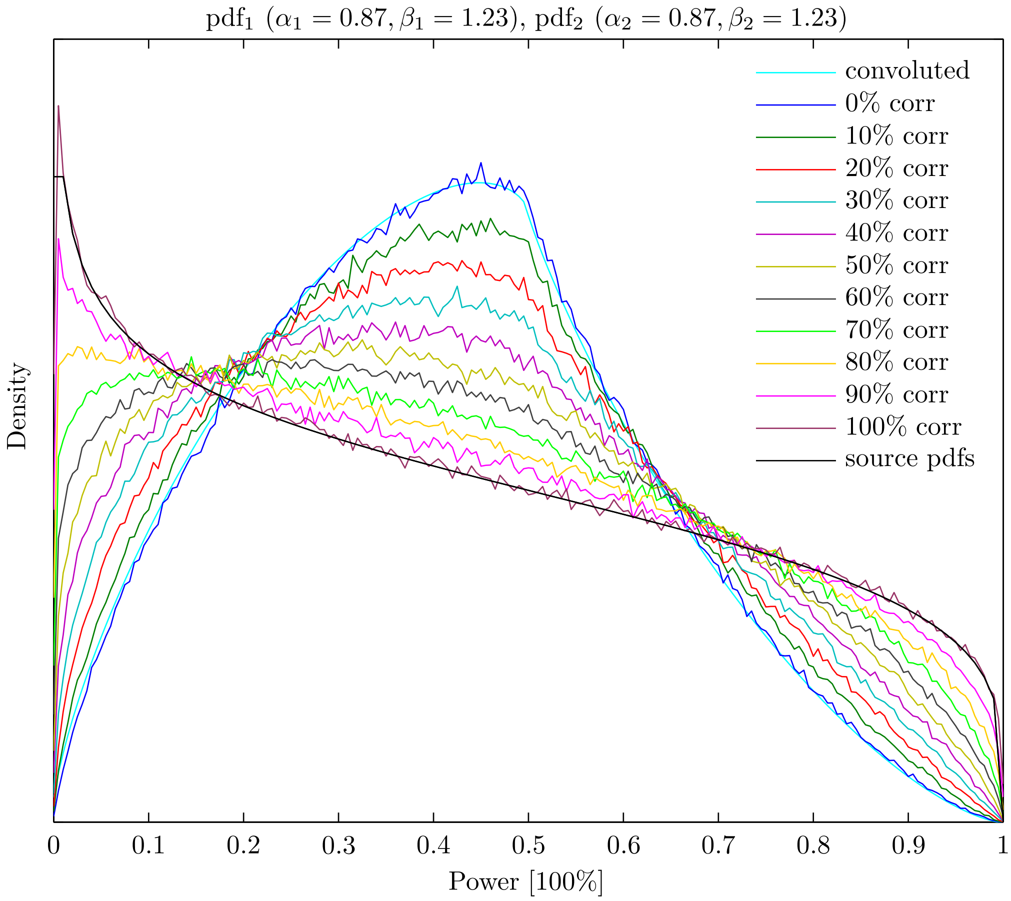

Fig. 8: Perfect positive correlation and distributions with same shape

2.5 Model

For our wind power output simulations, we defined an effective model consisting of three busses and three branches as can be seen in Fig. 9. W_1 and W_2 are wind power injections, S is the slack and L the load.

With this model we are able to answer the correlation questions as shown above. All the injected wind power flows through branch 1 and 2 to bus A. The slack compensates the imbalance between generation and load. On branch 1 and 2 we see the additive combination of both of the wind power injections and on branch 3 the flows are oppositely orientated.

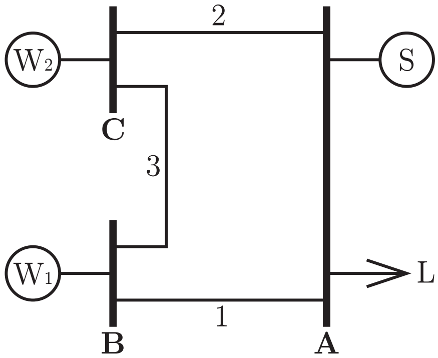

Fig. 9: 3 bus/3 branch test system with two wind power injections

2.6 Load Flow for Correlated Wind Power

For our power flow simulations we used the model shown in Fig. 9 and the wind power injections shown in Fig. 10. The distributions for the wind power injection are generated with real parameters from [8]. The load profile is from [15] from the year 2010 and is shown in Fig. 11. The best fit for this

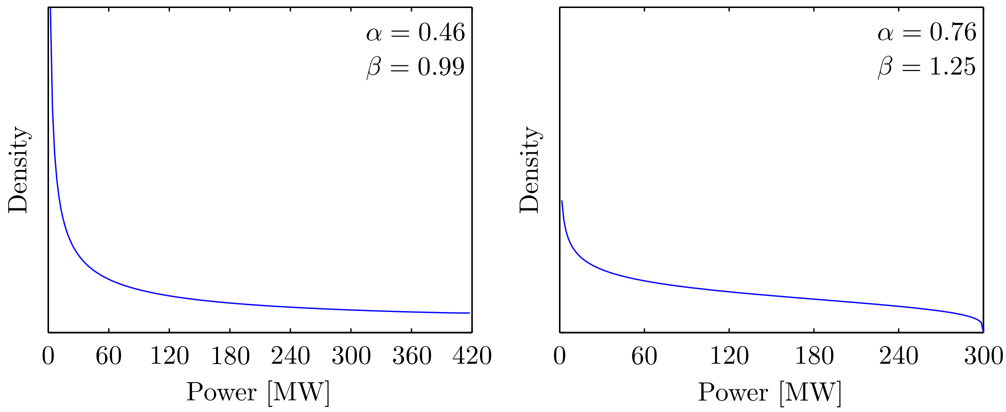

(a) Wind power injection W_1 on bus B (b) Wind power injection W_2 on bus C

Fig. 10: Probability density functions of wind power injections

profile is a Weibull distribution with scale parameter $\lambda = 1.75$ and shape parameter $k = 2.60$ for our time series generation. With this setup and our compensated generation of correlated random variables we are able to simulate the power flow with *DC Load Flow* method.

In the figures 12-14 we see the results for all three branches of our model. Fig. 12 shows branch 1 connecting bus A and bus C. This is one of the two transmission lines between generation and load side. The values are negative because the flow direction is defined from the lower bus number (A) to the

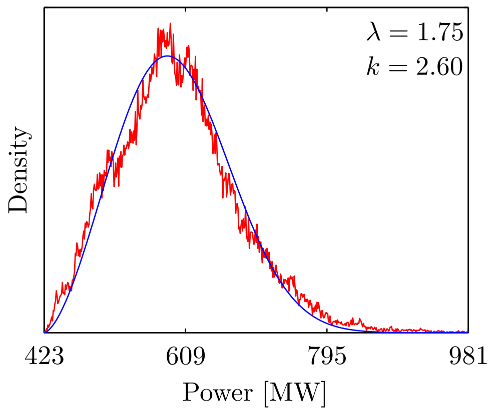

Fig. 11: Load profile

higher one (B). The physical flow is from bus B (generation) to bus A (load). With the β-distributions for wind power injection only a correlation less than 70 % can be obtained. On the next three images we see how the PDF changes for specific correlation levels. It can clearly be seen that the values of flow between 260 MW and 360 MW occur more often the higher the correlation level is. This means that the transmission line should have a higher capacity as in the case of no correlation. The same is valid for branch 2 (Fig. 13) but here the range is between 220 MW and 350 MW.

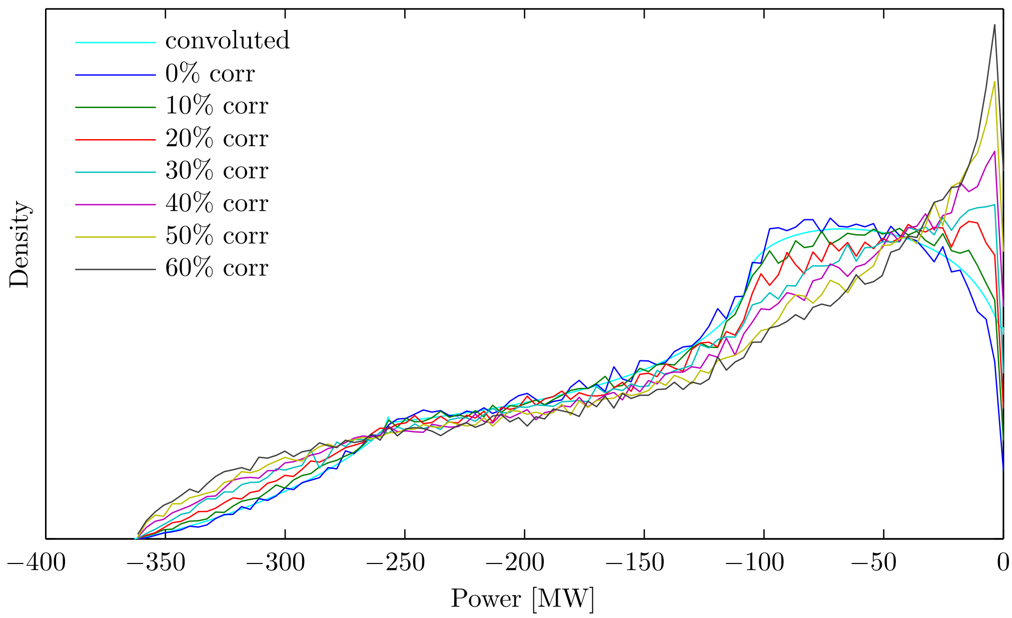

Fig. 12: Simulation result for branch 1

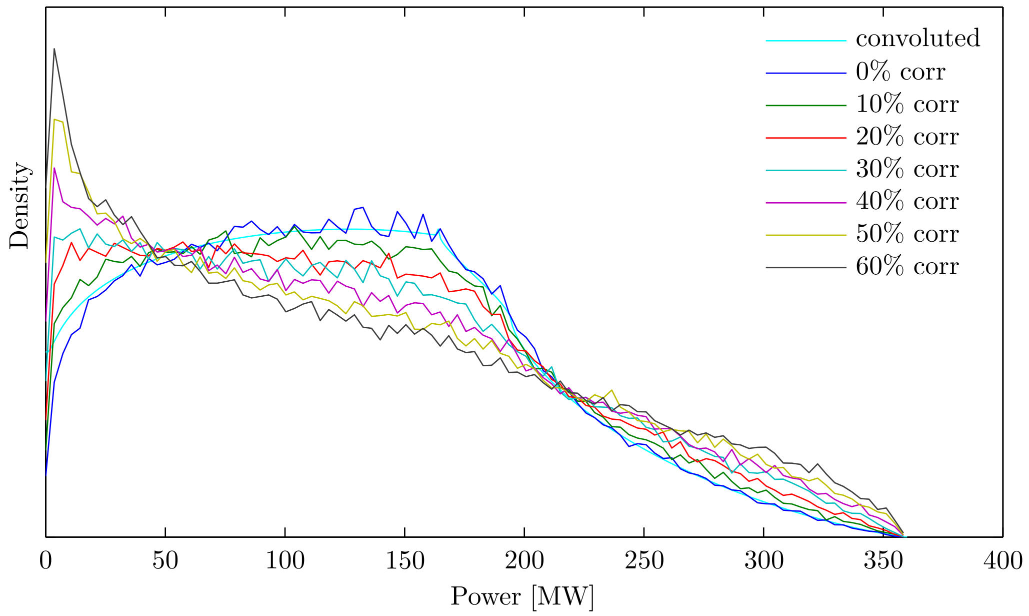

Fig. 13: Simulation result for branch 2

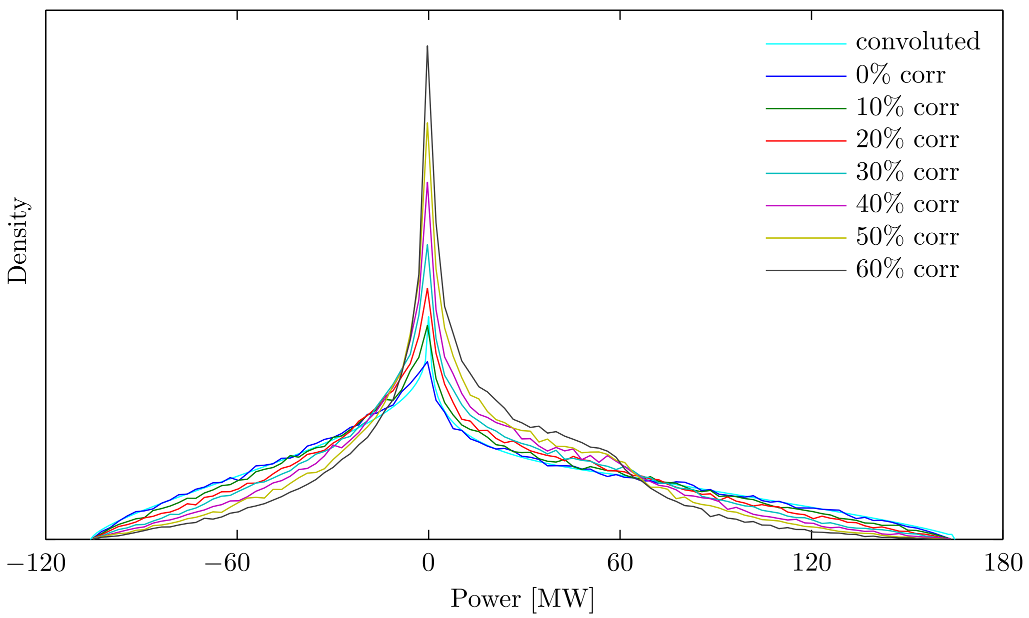

Fig. 14: Simulation result for branch 3

Branch 3 (Fig. 14) is completely different. Here we have flows in both directions. These flows partly compensate each other so we have a maximum at zero. The higher the correlation is the higher the maximum and rarer the larger power flow values are. This means the higher the correlation is the lower the capacity of line 3 can be.

2.7 Line Limit with Storage Usage

As additional feature of our simulations we can take line limits of the transmission lines into account. We considered a line limit of 320 MW for both transmission lines for the following simulations. At the injection side of each line a storage device is located. These storage devices are being charged with the surplus of energy of each line.

The PDFs of the lines are shown in Fig. 15 and Fig. 16. We can see that there is a peak at the limit. All absolute values above are cut off at the limit and so each larger value is mapped to this value. The curve for the convolution method is shown as reference.

In Fig. 17 a and Fig. 17 b the PDFs of the storage devices are shown. The peak at zero is not displayed. The presented curves are exactly the part that is cut off from the lines. With this method we can simulate the PDFs of charging the storage but not of the state of charge (SoC), therefore we need real data instead of generated time series.

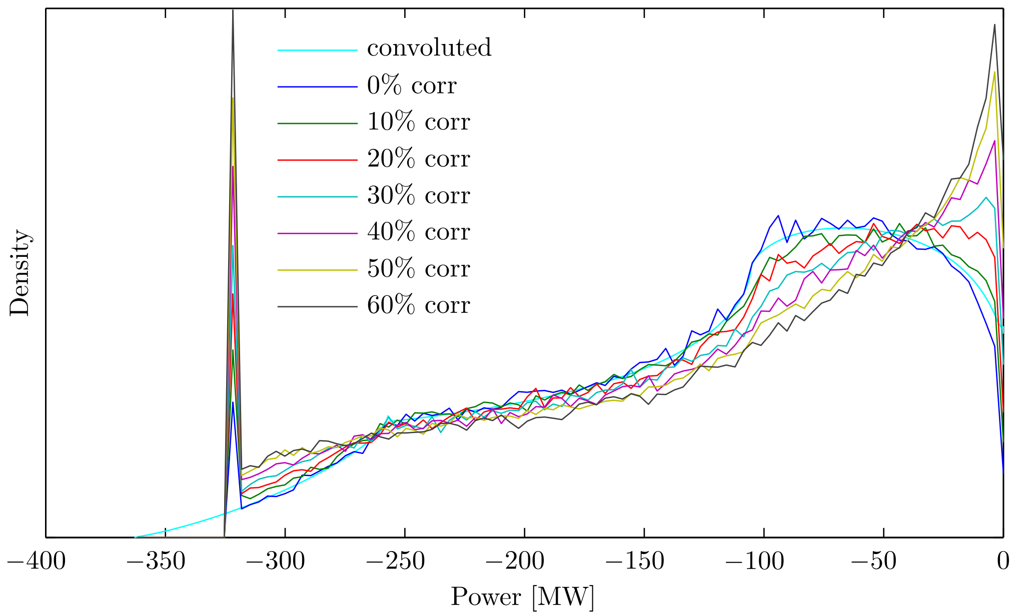

Fig. 15: Simulation result for branch 1 with line limit at 320 MW

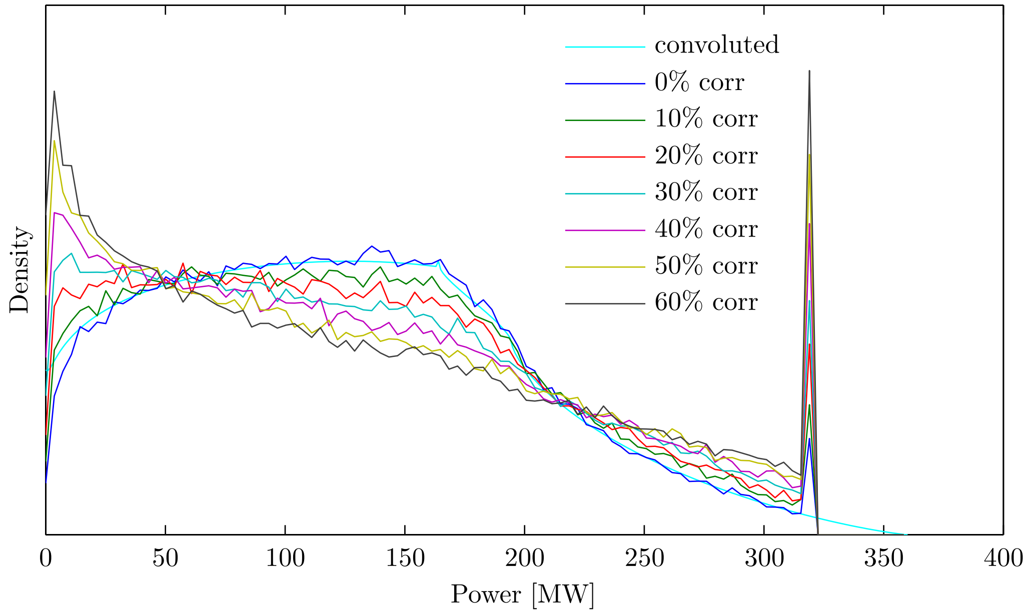

Fig. 16: Simulation result for branch 2 with line limit at 320 MW

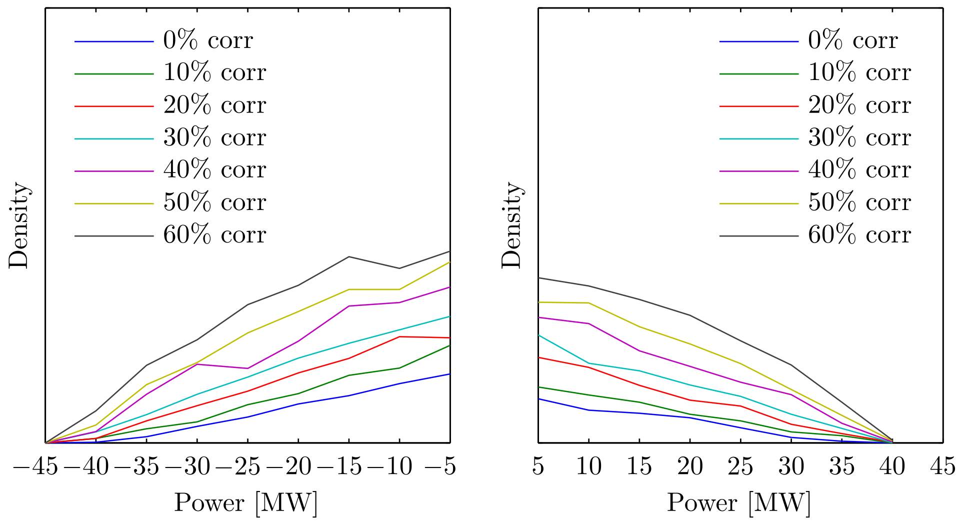

(a) Pdf of charging storage at branch 1 (b) Pdf of charging storage at branch 2

Fig. 17: Probability density functions of storage devices at the injection side

3 Real Data with Storage Usage

We also simulated storage use with real data so we were able to look at the SoC. We used the real wind data sets from BPA [15] with resolution of five minutes for a year. After error detection and removal we used the data set of 2008 for power injection at bus A, 2009 for bus B and 2010 for bus C. For bus E we used the load data set from 2008.

3.1 Model

For our simulations, we used the lower part of the IEEE 14 bus test system [16] with 5 buses and 7 branches. We adapted the test system for our needs and specified the generators as wind turbines. We added a third one at bus C and placed a storage device to each wind turbine. We canceled the loads at bus B and C and changed the load at bus E to the slack.

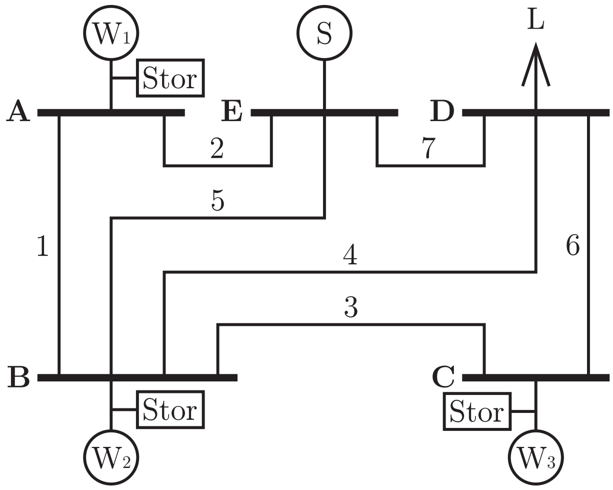

Fig. 18: Adapted lower part of IEEE 14 bus test system [16]

3.2 Simulations

In the real data simulations, we looked at the SoC of the storage devices at the wind power injection busses. We varied the time intervals from five minutes up to one year. With these simulations we figured out how the size of the storage must be in each case and what amount of energy has to be charged at the beginning. We can simulate two different storage usage modes. One is to use the storage as a buffer to achieve a net constant wind output and the other one for a constant slack usage over a specified time frame. In Fig. 19 we see the storage curves for a theoretical one year time frame for a constant wind output. The amount of energy is of course enormously high. A similar result is shown in Fig. 20 for a constant slack output. The amount

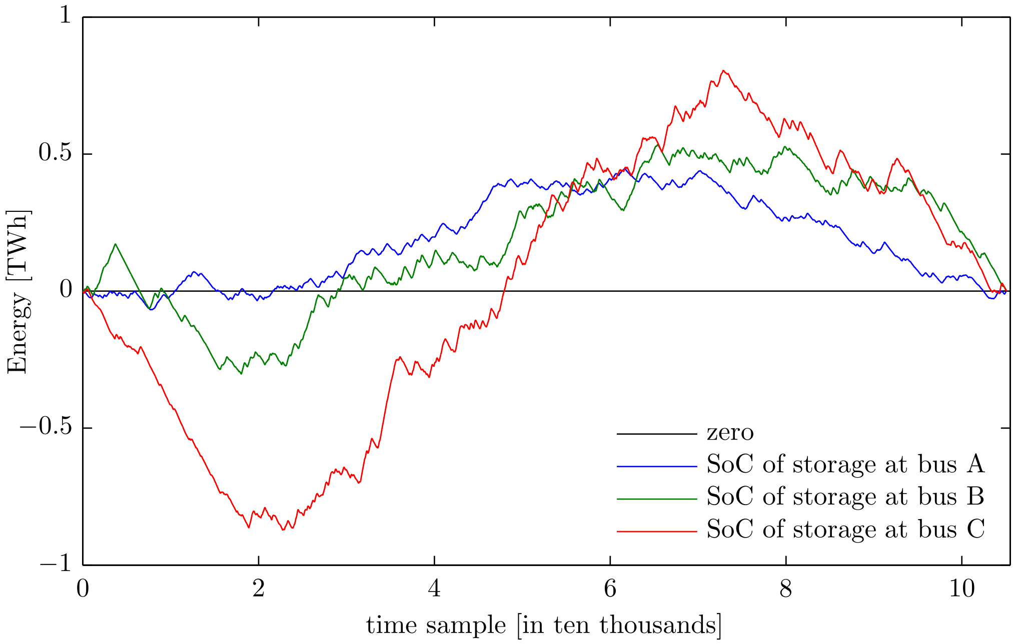

Fig. 19: SoC of storage units for a 1 year time frame for constant wind output

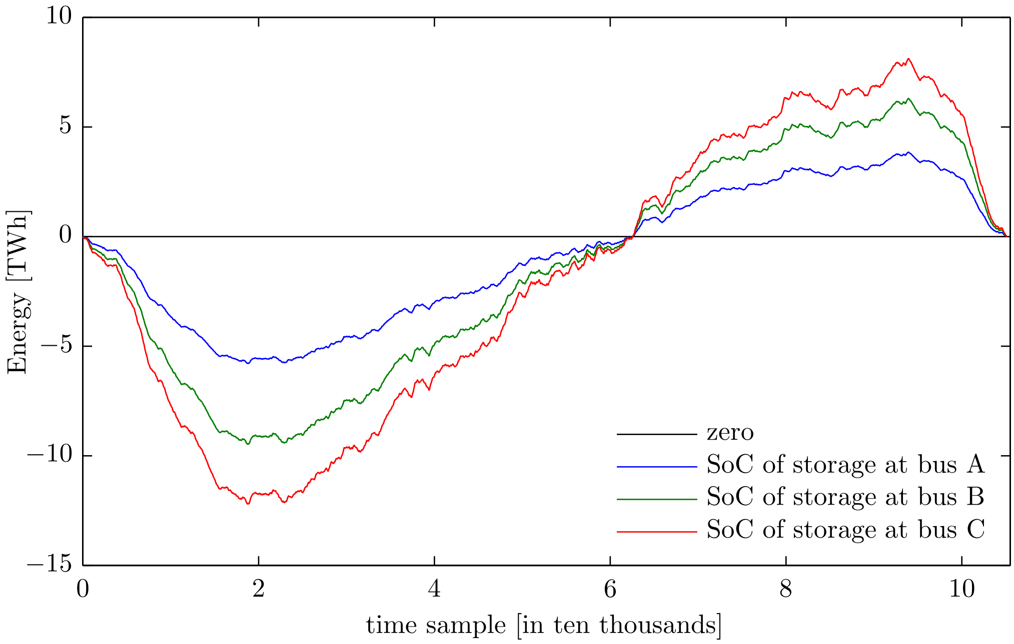

Fig. 20: SoC of storage units for a 1 year time frame for constant slack output

of energy needed is more than one decimal power higher than for a constant wind power output. For constant wind power output the bandwidth is only as wide as the maximum of power output is and the slack follows the load profile with an offset of the wind output. When trying to keep the slack constant the storage has to deal with the offset load profile.

The shorter the time frame is the lower is the needed amount of energy for the storage. For a 10 minutes time frame the needed storage size is around 50 MWh with some peaks up to 100 MWh and a couple of outliers up to 340 MWh for the constant slack case. For constant wind the average needed storage size is about 5 MWh with some peaks up to 15 MWh and a couple of outliers up to 25 MWh.

In Fig. 21 the PDFs of the storage devices are shown for the 1 year case. Fig. 21 a shows the PDFs for the constant wind case. The shapes are very similar to β-distributions and they are typically for wind power outputs. Due to the frequent occurrence of low values a high amount of negative power (power from the storage) is needed to achieve the constant value. In Fig. 21 b we see that the storage does not have to deal very often with large absolute values of power to balance wind. The PDF is relatively symmetrically.

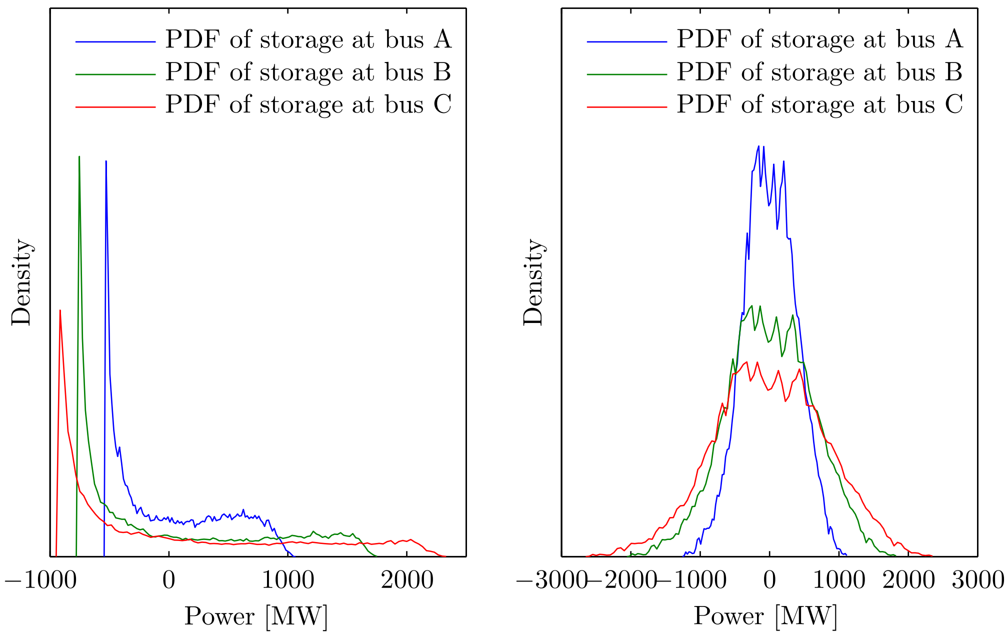

(a) PDFs for constant wind output (b) PDFs for constant slack output

Fig. 21: Probability density functions of storage devices

4 Conclusion

Based on [14], a modified method for generating correlated β-distributed random variables with bias compensation is proposed. Our achieved correlation is very close to the desired one. We applied a set of random variables spread from 0 % to 100 % correlation to our PLF simulations as input and derived a set of corresponding PDFs of each line flow as output. We showed how the PDF transforms from none to total correlation for each line. We also took line limits into account and used storage to avoid overload. Finally we used real data to simulate the storage size and initial charge level as well as the state of charge for storage devices located at the injection buses.

5 Acknowledgement

This research has been carried out at the department of Electrical and Computer Engineering within the Electrical Energy Systems Group at Carnegie Mellon University in Pittsburgh (PA), USA. This work has been done during a stay abroad at Carnegie Mellon University. The home institution is the institute of Energy Systems and Electrical Drives at Vienna University of Technology, Austria. It has been mainly financially supported by the Austrian Marshall Plan Foundation within the *Marshall Plan Scholarship*-program. This work also has been partially supported by the federal state of Lower Austria.

References

[1] OECD. *World Energy Outlook 2010*. OECD Publishing, 2010.

[2] Global Wind Energy Council. Global Wind Report - Annual market update 2010. `http://www.gwec.net/fileadmin/images/Publications/GWEC_annual_market_update_2010_-_2nd_edition_April_2011.pdf`, April 2011.

[3] G. Brauner. *Vorlesungsunterlagen zu Energieversorgung*. Vienna University of Technology, 2006.

[4] Xu Lu, Michael B. McElroy, and J. Kiviluoma. Global potential for wind-generated electricity. *Proceedings of the National Academy of Sciences*, 2009.

[5] B. Borkowska. Probabilistic load flow. *Power Apparatus and Systems, IEEE Transactions on*, PAS-93(3):752–759, may 1974.

[6] P. Chen, Z. Chen, and B. Bak-Jensen. Probabilistic load flow: A review. In *Electric Utility Deregulation and Restructuring and Power Technologies, 2008. DRPT 2008. Third International Conference on*, pages 1586–1591, april 2008.

[7] H. Louie. Evaluation of probabilistic models of wind plant power output characteristics. In *Probabilistic Methods Applied to Power Systems (PMAPS), 2010 IEEE 11th International Conference on*, pages 442–447, June 2010.

[8] H. Louie. Characterizing and modeling aggregate wind plant power output in large systems. In *Power and Energy Society General Meeting, 2010 IEEE*, pages 1–8, July 2010.

[9] N.L. Johnson, S. Kotz, and N. Balakrishnan. *Continuous Univariate Distributions*, volume 2 of *Wiley series in probability and mathematical statistics. Probability and mathematical statistics.* Wiley & Sons, New York, second edition, 1995.

[10] B.W. Lindgren. *Statistical Theory.* Texts in Statistical Science Series. Chapman & Hall, 1993.

[11] C.T. Dos Santos Dias, A. Samaranayaka, and B. Manly. On the use of correlated beta random variables with animal population modelling. *Ecological Modelling*, 215(4):293 – 300, 2008.

[12] J. Usaola. Probabilistic load flow with correlated wind power injections. *Electric Power Systems Research*, 80(5):528 – 536, 2010.

[13] M. Catalani. Sampling from a couple of positively correlated beta variates. *Arxiv*, pages 1–7, 2002.

[14] S. Magnussen. An algorithm for generating positively correlated beta-distributed random variables with known marginal distributions and a specified correlation. *Computational Statistics & Data Analysis*, 46(2):397–406, 2004.

[15] Bonneville Power Administration. BPA Balancing Authority Load & Total Wind Generation. `http://transmission.bpa.gov/Business/Operations/Wind/default.aspx`, July 20, 2011.

[16] IEEE. IEEE 14 Bus Test Case. `http://www.ee.washington.edu/research/pstca/pf14/pg_tca14bus.htm`, July, 20 2011.